

Attention-Guided Autoencoder for Automated Progression Prediction of Subjective Cognitive Decline with Structural MRI

Hao Guan, Ling Yue, Pew-Thian Yap, Andrea Bozoki, Mingxia Liu, *Senior Member, IEEE*

Abstract—Subjective cognitive decline (SCD) is a preclinical stage of Alzheimer’s disease (AD) which occurs even before mild cognitive impairment (MCI). Progressive SCD will convert to MCI with potential of further evolving to AD. Therefore, early identification of progressive SCD with neuroimaging techniques (e.g., structural MRI) is of great clinical value for early intervention of AD. However, existing MRI-based machine/deep learning methods usually suffer the small-sample-size problem which poses great challenge to related neuroimaging analysis. The central question we aim to tackle in this paper is how to leverage related domains (e.g., AD/NC) to assist the progression prediction of SCD. Meanwhile, we are concerned about which brain areas are more closely linked to the identification of progressive SCD. To this end, we propose an attention-guided autoencoder model for efficient cross-domain adaptation which facilitates the knowledge transfer from AD to SCD. The proposed model is composed of four key components: 1) a feature encoding module for learning shared subspace representations of different domains, 2) an attention module for automatically locating discriminative brain regions of interest defined in brain atlases, 3) a decoding module for reconstructing the original input, 4) a classification module for identification of brain diseases. Through joint training of these four modules, domain invariant features can be learned. Meanwhile, the brain disease related regions can be highlighted by the attention mechanism. Extensive experiments on the publicly available ADNI dataset and a private CLAS dataset have demonstrated the effectiveness of the proposed method. The proposed model is straightforward to train and test with only 5~10 seconds on CPUs and is suitable for medical tasks with small datasets.

Index Terms—Subjective Cognitive Decline, Alzheimer’s disease, domain adaptation, structural MRI, autoencoder, attention mechanism

I. INTRODUCTION

As one of the main causes of dementia and death, Alzheimer’s disease (AD) has affected millions of elderly people around the world [1]. As illustrated in Fig. 1, AD is characterized as a chronic neurodegenerative process with an extended spectrum to an earlier stage even before its prodromal stage (*i.e.*, mild cognitive impairment, MCI), termed as subjective cognitive decline (SCD) or subjective

H. Guan, P.-T. Yap and M. Liu are with the Department of Radiology and Biomedical Research Imaging Center, University of North Carolina at Chapel Hill, Chapel Hill, NC 27599, USA. L. Yue is with the Department of Geriatric Psychiatry, Shanghai Mental Health Center, Shanghai Jiao Tong University School of Medicine, Shanghai 200030, China. A. Bozoki is with the Department of Neurology, University of North Carolina at Chapel Hill, NC 27599, USA. Corresponding author: M. Liu (mxliu@med.unc.edu).

This work was supported in part by NIH grant (Nos. RF1AG073297 and R01AG041721).

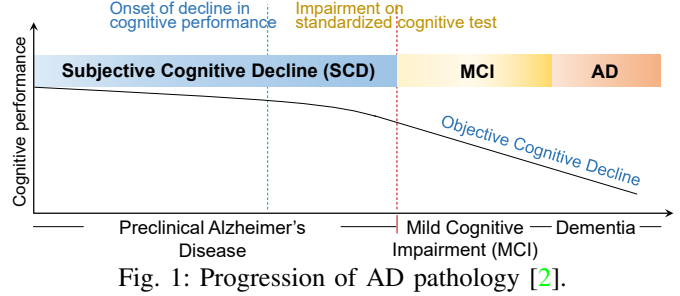


Fig. 1: Progression of AD pathology [2].

memory complaint (SMC) [2], [3]. Growing evidences have shown that individuals with SCD may suffer an increased risk of underlying AD pathology. Thus progression prediction of SCD is of great clinical value for early intervention of the brain disease progress. Neuroimaging has been shown as an effective technology to understand the underlying neuropathological mechanisms of brain diseases and has already been used for identification of SCD [4], [5].

Structural magnetic resonance imaging (sMRI) is one of the most commonly used imaging modalities for AD-spectrum identification [6], [7]. As the preclinical stage of AD, it typically takes several years for a progressive SCD subject to evolve to MCI, which makes the data collection a time-consuming and challenging task. Although several previous studies have applied machine learning to MRI-based SCD progression prediction [8]–[11], they usually suffer from the small-sample-size problem. Thus how to solve the small-sample-size problem for SCD and develop an effective machine learning system with good generalization ability is of practical clinical value. An intuitive solution may be data augmentation or data synthesis [12], [13]. However, it heavily depends on the original training data which greatly limits their capability and flexibility.

We observe that there are relatively much more number of AD and Normal Control (NC) subjects in real-world practice. How to transfer the knowledge from existing AD/NC subjects for SCD progression prediction task is the key question we aim to answer in this paper. With the fact that AD is a chronic neurodegenerative process, we assume that there are potential relationships between AD and SCD, and both of them can be represented in a shared latent feature space. In addition, we are interested in finding important brain regions-of-interest (ROI) that are associated with SCD. This is helpful to enable the computer-aided diagnosis system more interpretable.

Based on these motivations, we propose an attention-guided autoencoder for cross-domain adaptation with application on SCD progression prediction. Our model consists of four key components: 1) a feature encoding module for learning shared subspace representations of different domains, 2) an attention module for automatically finding discriminative brain regions of interest defined by brain atlases, 3) a decoding module for reconstructing original input, 4) a classification module for identification of brain diseases. During training, the input MR images (in terms of features, *e.g.*, ROI) are first squeezed into a low-dimensional subspace through the feature encoding module. The reconstruction model enables the intermediate subspace representations informative to represent the input data. Meanwhile, the classification module enforces the learned representation to be disease-discriminative. Through the joint training of reconstruction and classification, domain invariant features can be learned.

This work makes the following contributions. 1) We propose an attention-guided autoencoder for efficient cross-domain adaptation which is applied to MRI-based SCD progression prediction. 2) We incorporate an attention mechanism which enables our model to automatically identify disease-related brain regions with good interpretability.

The rest part of this paper is organized as follows. We first review related studies in Section II. Section III introduces the materials adopted in this work. Section IV introduces the proposed method in details. In Section V, we present the experimental settings, evaluation metrics, competing methods and experimental results. We further analyze the brain ROIs highlighted by the model and influence of several key parameters of the proposed method in Section VI. The paper is finally concluded in Section VII.

II. RELATED WORKS

A. Learning-based SCD Progression Prediction

As a preclinical stage of AD, SCD has attracted a growing awareness in the field of brain disease analysis. Existing studies on SCD can be roughly divided into non-neuroimaging-based methods and neuroimaging-based methods. Engedal *et al.* [14] explore the use of electroencephalography (EEG) with statistical method to predict SCD conversion. Engedal *et al.* [15] use demographic information through machine learning to predict the progression of SCD. Since structural MRIs have been widely applied in computer-aided brain disorder diagnosis, numerous machine learning methods have been proposed to deal with AD-related brain disorder classification [16], [17]. Yue *et al.* [8] utilize cost sensitive support vector machine (CSV) for SCD progression prediction based on a combination of clinical and MRI features. Felpete *et al.* [9] use SVM and random forest for prediction of SCD conversion. Lin *et al.* [10] introduce sparse-coding for MRI feature selection and use random forest for SCD identification. Liu *et al.* [11] propose a GAN-based framework to synthesize PET and MRI data of SCD which can enhance the training data and assist SCD progression prediction. Despite these progress, identifying progressive SCD (pSCD) and stable SCD (sSCD) individuals is still a very challenging task due to the

small-sample-size problem and insignificant pathological brain changes. Since SCD is a preclinical stage of AD, how to leverage the knowledge from AD/NC classification task (with relatively large amount of labeled samples, and significant pathological brain changes) to SCD progression prediction is an important and open problem with clinical value.

B. Domain Adaptation for AD-related Disease Identification

Recently transfer learning [18]–[20] or domain adaptation [21], [22] has become a promising tool in medical imaging to tackle the problem when the target domain has relatively small amount of data and different distribution from the source domain. These methods do not require identical distribution of the training data (source domain) and test data (target domain) and can share knowledge between different domains. Some previous studies propose to use transfer learning for early diagnosis of AD. Cheng *et al.* [23], [24] propose a domain transfer support vector machine (DTSVM) for MCI conversion prediction. A cross-domain kernel learning module is trained with auxiliary domain (AD/NC) and MCI samples, and then used to build a transferable SVM. With the recent progress of deep learning (DL), some methods leverage deep neural network through fine-tuning to facilitate transfer learning for AD-related classification [25], [26]. Lian *et al.* [27] reveal that training a deep convolutional neural network with AD/NC samples is beneficial for MCI conversion prediction. These transfer learning-based methods indicate that brain changes from cognitively normal to AD are potentially related to its early stages, which is consistent with the fact that AD is a progressive neurodegenerative disease. Therefore, knowledge learned from AD/NC data can be used to identify SCD progress. Despite the effectiveness, all these methods need label information from the target data, limiting their utility in unsupervised problems.

III. MATERIALS

A. Data Acquisition

We employ T1-weighted structural MRIs from two datasets in this work for model training and test. The first one is the publicly available brain MR dataset, *i.e.*, Alzheimer’s Disease Neuroimaging Initiative (ADNI) [6]¹. We use 3T T1-weighted structural MRIs of 159 AD patients and 201 normal controls (NCs) from the ADNI dataset in this work.

The second dataset is the Chinese Longitudinal Aging Study (CLAS) dataset [28]. It consists of 3T T1-weighted structural MRIs acquired from 76 SCD subjects. These SCD subjects are categorized into progressive SCD (pSCD) and stable SCD (sSCD). There are totally 24 pSCD subjects that have converted to MCI within 84 months, while 52 sSCD subjects keep stable. The demographic information of the datasets are shown in Table I.

B. Image Preprocessing

All the T1-weighted MRIs are preprocessed through a standard pipeline, including 1) skull stripping, 2) intensity

¹<https://ida.loni.usc.edu>

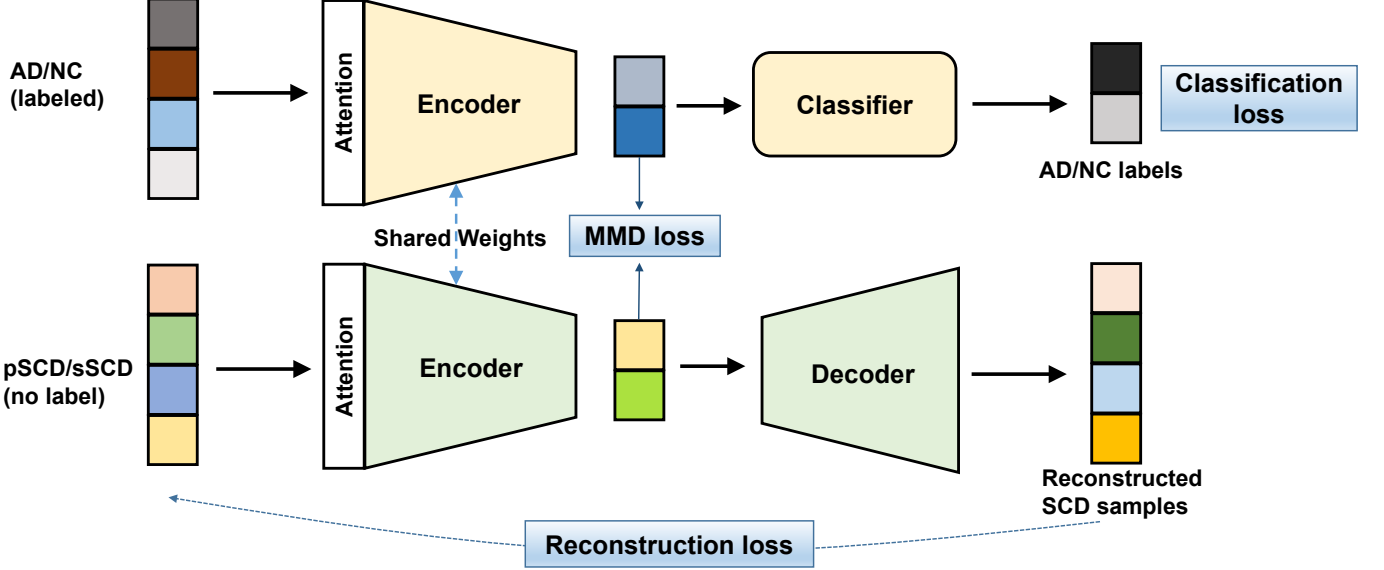


Fig. 2: Illustration of the main framework of the proposed model for MRI-based SCD progression prediction.

TABLE I: Demographic information of the subjects for SCD progression prediction. The values are denoted as “mean \pm standard deviation”. F/M: Female/Male.

Dataset	Category	Gender (F/M)	Age	MMSE
ADNI	AD	67/92	74.4 \pm 8.1	23.1 \pm 2.2
	NC	105/95	73.4 \pm 6.2	29.0 \pm 1.3
CLAS	pSCD	13/11	71.3 \pm 6.6	26.8 \pm 2.6
	sSCD	27/25	68.6 \pm 7.2	27.7 \pm 2.2

inhomogeneity correction, 3) registration to the Automated Anatomical Labeling (AAL) template [29], and 4) re-sampling to the resolution of $1 \times 1 \times 1 \text{ mm}^3$. We use Freesurfer² to facilitate skull stripping, and adopt the SPM software package³ to conduct the other MRI preprocessing steps. After being processed, all the MRIs have the identical dimension of $181 \times 217 \times 181$.

C. Features Extraction

For statistical analysis and model training, we extract the ROI features from the structural brain MRIs. It is calculated by the gray matter volumes of 90 regions defined in the AAL brain atlas⁴. The advantage of ROI features is they contain prior knowledge from neuroscientists and have good interpretability for indicating which brain areas are more closely related to the disease classification. The dimension of ROI feature in this work is 90.

IV. METHODOLOGY

A. Problem Formulation

In this paper, we leverage unsupervised domain adaptation for SCD progression prediction. Let $\mathcal{X} \times \mathcal{Y}$ denote the feature

space of samples and their corresponding labels. A source domain \mathcal{D}_S and a target domain \mathcal{D}_T are defined on the feature space, but have different distributions. Suppose there are n_s samples with category labels in the source domain, *i.e.*, $\mathcal{D}_S = \{(\mathbf{x}_i^S, y_i^S)\}_{i=1}^{n_s}$, while n_t samples in the target domain without category labels, *i.e.*, $\mathcal{D}_T = \{(\mathbf{x}_j^T)\}_{j=1}^{n_t}$. These two domains share the same set of category labels. In our work, AD/NC samples are set as the source domain (AD: 1, NC: 0), while pSCD/sSCD samples are the target domain (pSCD: 1, sSCD: 0). The goal here is to train a model with labeled source domain samples and unlabeled target domain samples, so that the learned model can generalize well to target data for label estimation.

B. Main Structure of Attention-Guided Autoencoder

Fig. 2 illustrates the main structure and workflow of the proposed model for cross-domain adaptation and prediction. As shown in Fig. 2, the model consists of four key components. 1) The attention module automatically selects and highlights the most discriminative features of the input data. For brain ROI features, it can help locate which regions are more disease-related. 2) The encoder module projects the input data from original feature space to a latent compressed feature space. 3) The decoder module reconstructs the input data from the intermediate compressed representations to its original feature space. 4) The classifier predicts the class label with the intermediate compressed representations. In the training phase, the source data and target data (in terms of feature vectors) first go through the attention module for “feature filtering”. Then the data are fed into the encoder module and projected into a low-dimension latent feature space. A maximum mean discrepancy (MMD) loss is facilitated on these compressed representations of source and target data to reduce their domain difference. With the compressed representations, a classifier is trained with the category labels (source domain) to enforce the projected latent features more discriminative

²<https://surfer.nmr.mgh.harvard.edu/>

³<https://www.fil.ion.ucl.ac.uk/spm/>

⁴<https://www.gin.cnrs.fr/en/tools/aal/>

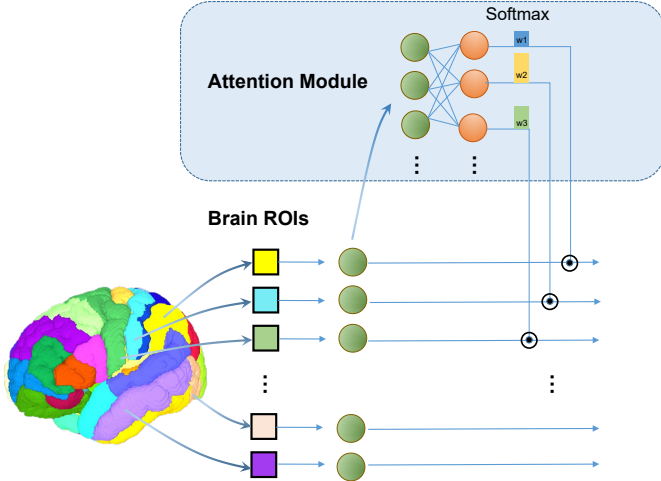


Fig. 3: Illustration of the attention module of the proposed model for SCD progression prediction.

to brain disorders. Meanwhile, a decoder is trained using reconstruction loss to enforce the projected latent features contain the most useful information within the target data.

In the test stage, the trained classifier is directly applied to the target domain (SCD) for the prediction of the class labels (pSCD vs. sSCD).

C. Attention Mechanism

According to previous studies, brain disorders are highly associated with certain brain regions [30]–[33]. Since we use brain ROI feature as the input, we aim to automatically identify which regions are more disease-related. This can also enhance the interpretability of the entire model which is important for medical image analysis. As illustrated in Fig. 3, the 90-dimensional ROI feature is adopted the input of the network, denoted as $I = (R_1, R_2, \dots, R_n)$. The feature is fed into an attention network which consists 90 neurons. Softmax is used as the activation function. The softmax function can output a probability (weight) on each dimension of the 90-dimension feature with a summation of 1, *i.e.*, $\mathbf{w} = [w_1, w_2, \dots, w_n], \sum_{i=1}^n w_i = 1$. These weights are then multiplied with the original input ROI feature to get weighted features. From the output probabilities of the attention module, we can analyze the importance of different brain regions.

D. Feature Encoding and Adaptation

After feature importance weighting by the attention module, the source and target data are fed into the feature encoder. The feature encoder projects the data into a low-dimensional latent space. To achieve this, we design a three-layer multiple-layer-perception (MLP) with 90, 64, 32 neurons, respectively. After encoding, all the data have been projected to the 32-dimensional space. The encoders for the source and target data share the same weights. To align the feature distributions of source and target data in the projected space, we adopt

maximum mean discrepancy (MMD) loss which is defined as follows:

$$\text{MMD}_k^2 = \|\mathbf{E}_p[\phi(\mathbf{x}^s)] - \mathbf{E}_q[\phi(\mathbf{x}^t)]\|_{\mathcal{H}_k}^2 \quad (1)$$

where \mathcal{H}_k represents the Reproducing Kernel Hilbert Space (RKHS) endowed with a kernel function k , and $k(\mathbf{x}^s, \mathbf{x}^t) = \langle \phi(\mathbf{x}^s), \phi(\mathbf{x}^t) \rangle$.

Through minimizing the MMD loss, the source and target data distributions in the latent feature space can be aligned.

E. Joint Classification and Reconstruction for Adaptation

In our model for cross-domain adaptation, the encoder module plays the role of learning domain-sharing features. To this end, the training of the encoder should be driven by tasks with certain supervisions. For AD/NC samples, due to the their relatively large amount and abundant label information, a classification module is trained with these labeled source data with the cross-entropy loss as:

$$\mathcal{L}_{cls} = \sum_{i=1}^N -y_i \ln(\hat{y}_i) - (1 - y_i) \ln(1 - \hat{y}_i) \quad (2)$$

where y_i is the label (0, 1) and \hat{y}_i is the output of network (classification module).

For the target data, *i.e.*, SCD samples, since there is no label information (pSCD or sSCD) provided during training, we use the reconstruction loss as the supervision. Specifically, a decoder is linked to output of the encoder, and tries to reconstruct the original input target data. The decoder has a symmetric structure to the encoder, with 32, 64, 90 neurons each layer, respectively. We use \mathcal{L}_1 norm as the reconstruction loss defined as:

$$\mathcal{L}_{recon} = \sum_{i=1}^N \|\mathbf{x}_i^t - \hat{\mathbf{x}}_i^t\|_1 \quad (3)$$

where \mathbf{x}_i^t denotes the i -th sample in the target domain while $\hat{\mathbf{x}}_i^t$ is the corresponding reconstructed result by the decoder.

The classification module and the reconstruction module are trained jointly and they provide supervisions for the learning process. Through the joint training, the encoder can be enforced to learn features that are both discriminative to brain diseases and reflect information within the SCD data. It should be noted that the total number of target samples (SCD) is much smaller than the source data (AD/NC). To achieve joint training, the SCD samples must be enhanced. In our practice, we simply duplicate the SCD samples to make them has equal number with the source data. This can make both the classification and reconstruction modules be updated each training epoch. To avoid a bias towards the source data, the reconstruction loss for the target data can be allocated a relatively higher weight during training.

During training, the overall loss \mathcal{L} is calculated as:

$$\mathcal{L} = \lambda_1 \mathcal{L}_{mmd} + \lambda_2 \mathcal{L}_{cls} + \mathcal{L}_{recon} \quad (4)$$

where λ_1 and λ_2 are the parameters to control the contributions of the three terms in Eq. (4).

F. Implementation

The proposed model is implemented using PyTorch. The Adam algorithm is utilized as the optimizer with a learning rate of 0.001. A linear kernel is adopted as the kernel function for the MMD loss in Eq. (1). The parameters λ_1 and λ_2 in Eq. (4) are set to 0.1 and 0.1, respectively. The proposed model is trained for 60 epochs with the batch size of 100. The overall training and test take around 5~10 seconds with reproducible results.

V. EXPERIMENT

A. Experimental Setup

In our experiment, we adopt the ADNI dataset as the source domain, while the CLAS dataset as the target domain. The model architecture keeps fixed throughout the experiment.

To evaluate the performance of different methods, we utilize five metrics in the experiments, *i.e.*, classification accuracy (ACC), balanced accuracy (BAC), sensitivity (SEN), specificity (SPE), and area under the receiver operating characteristic curve (AUC). Denote TP, TN, FP, FN as the true positive, true negative, false positive and false negative, respectively. Then these five evaluation metrics are defined as $ACC = \frac{TP+TN}{TP+TN+FP+FN}$, $SEN = \frac{TP}{TP+FN}$, $SPE = \frac{TN}{TN+FP}$, and $BAC = \frac{SEN+SPE}{2}$. For each evaluation metric, a higher value indicates a better classification performance.

B. Competing Methods

We compare the proposed method with the following six methods, including one baseline method, three statistical learning-based methods, and a deep learning-based method.

(1) **Baseline.** This method uses logistic regression, one of the most popular classification model in neuroimaging analysis [34]–[36] for structural MRI-based SCD progression prediction. It is trained on the AD/NC samples from ADNI, and then applied to CLAS for pSCD/sSCD classification.

(2) **Transfer component analysis (TCA)** [37]. In this method, several transfer components are learned across domains in the reproducing kernel Hilbert space using maximum mean discrepancy (MMD). In TCA, source and target data are both projected to the subspace spanned by these transfer components. After that, a logistic classifier trained with source data (AD/NC) is used to facilitate pSCD/sSCD classification in the projected feature space. In our experiments, a linear kernel is adopted for feature learning in TCA. We set the subspace dimension of TCA to 40, $\lambda = 0.01$, $\gamma = 0.1$, respectively.

(3) **Geodesic flow kernel (GFK)** [38]. In this method, a domain specific n-dimensional subspace is calculated for the source and target data. Then the source and target data are projected into an intermediate subspaces along the shortest geodesic path connecting these two n-dimensional subspaces on the Grassmann manifold. After adaptation, a logistic classifier is adopted to conduct pSCD/sSCD classification using these projected data. In our experiment, the the subspace dimension in GFK is set to 20.

(4) **Subspace alignment (SA)** [39]. In this method, the source data is projected into the source subspace and the target

data is represented by target subspace. Both of them use their principal components as the subspace representation. Then a transformation matrix that maps the source subspace to the target one is learned to mitigate domain shift. After adaptation, a logistic classifier is built to do pSCD/sSCD classification using these projected data. The parameter for the subspace dimension in SA is set to 20.

(5) **Correlation alignment (CORAL)** [40]. In this method, domain shift is minimized through aligning second-order statistics of source and target domains. After adaptation, we adopt a logistic classifier for pSCD/sSCD classification using these aligned data. CORAL only calculates the covariance of source and target features without any additional parameters.

(6) **VoxCNN** [41]. VoxCNN is a deep 3D convolutional neural network designed for structural MRI-based dementia classification. It consists of ten $3 \times 3 \times 3$ convolution layers (with the filters numbers of 8, 8, 16, 16, 32, 32, 32, 64, 64, and 64, respectively) for automated feature learning, and two fully-connected layers for classification. We first train the VoxCNN with AD/NC samples from the ADNI dataset, then directly apply it for pSCD/sSCD classification on the CLAS dataset.

C. Results of SCD Progression Prediction

We conduct experiment on the ADNI and CLAS datasets for SCD progression prediction, *i.e.*, pSCD vs. sSCD classification. Label information of CLAS is not available during training. The performance of six different methods and our model is listed in Table II. From Table II, we have the following observations.

First, in terms of ACC and BAC, the baseline model has the inferior performance than the other competing methods. This indicates that domain shift among different domains can significantly affect a machine learning model. Meanwhile, the adaptation-based methods can achieve better results than the baseline which implies the effectiveness of domain adaptation for reducing domain shift.

Second, the proposed model outperforms the other methods by a large margin. This can be attributed to two reasons. 1) Most of the competing methods conduct adaptation through alignment of the source and target in an unsupervised way, *i.e.*, the label information of the source data is not utilized in the adaptation process. We argue that incorporating the label information is helpful to make the learned representation more discriminative to diseases. 2) The attention mechanism in our model can select more discriminative features for classification and enhance the training results.

D. Comparison with State-of-the-Arts

We further compare the proposed method with several state-of-the-art methods for structural MRI-based SCD progression prediction, including: 1) Cost-Sensitive SVM (CSVM) [8], 2) Random Forest [9] and 3) Generative Adversarial Network [42]. We reproduce these methods and conduct experiments of pSCD/sSCD classification on the same datasets for a fair comparison. The CSVM is implemented using an SVM with a linear kernel which is trained with the cost matrix $\begin{pmatrix} 0 & 10 \\ 1 & 0 \end{pmatrix}$. The RF is built through an ensemble of decision tree

TABLE II: Performance of seven different methods for SCD progression prediction (*i.e.*, pSCD vs. sSCD classification), as well as p -values via paired sample t -test between our method and each of competing methods.

Method	ACC (%)	BAC (%)	AUC (%)	SEN (%)	SPE (%)	$p < 0.05$
Baseline	57.89	54.65	58.17	45.83	63.46	Yes
TCA	60.53	59.94	55.85	58.33	61.54	Yes
GFK	59.21	57.85	58.81	54.17	61.54	Yes
SA	61.84	59.78	60.26	54.17	65.38	Yes
CORAL	59.21	60.10	56.01	62.50	57.69	Yes
VoxCNN	67.11	54.65	55.45	20.83	88.46	Yes
Ours	69.74	67.79	61.86	62.50	73.08	—

TABLE III: Performance of the proposed method and several state-of-the-arts for SCD progression prediction.

Method	Model	ACC (%)	BAC (%)	AUC (%)	SEN (%)	SPE (%)	$p < 0.05$
Yue <i>et al.</i> [8]	Cost-Sensitive SVM	53.95	56.25	51.52	62.50	50.00	Yes
Felpete <i>et al.</i> [9]	Random Forest	59.21	57.85	63.66	54.17	61.54	Yes
Liu <i>et al.</i> [42]	GAN	65.50	67.05	71.30	72.50	61.60	—
Ours	Attention Autoencoder	69.74	67.79	61.86	62.50	73.08	—

models. The GAN is composed of a generator (3 convolution layers, 3 residual blocks and 2 deconvolution layers) and a discriminator (5 convolution layers).

The prediction results are reported in Table III. From Table III, our method achieves better or comparable performance than the state-of-the-art methods. More specifically, our model achieves higher accuracy, balanced accuracy (*i.e.*, 69.74%, 67.79%) and specificity (*i.e.*, 73.08%) which are much better than the other three state-of-the-art methods, even though GAN is a complex deep-learning methods. Note that the GAN model utilizes both MRI and PET data with much more training data (both original and synthetic images) than ours, thus it achieves a higher SEN and AUC value. Despite this, our model still achieves comparable performance. Considering that the proposed model only takes 5~10 seconds on CPUs to train while the GAN typically takes several days, our model has made a good balance between accuracy and efficiency.

E. Application to MCI Conversion Prediction

We further evaluate the proposed model in the task of MCI to AD conversion prediction, *i.e.*, pMCI vs. sMCI classification. A total of 393 MCI subjects (167 pMCI, 226 sMCI) with structural MRIs are used as the unlabeled target domain, while AD/NC samples are adopted as the labeled source domain. The pMCI subjects would convert to AD within 36 months while sMCI would not. We still extract the ROIs features to represent each subject. The VoxCNN directly takes MRIs as the input for end-to-end training. It is firstly pre-trained with AD/NC samples then applied for MCI conversion prediction. The results of seven different methods for MCI conversion prediction is reported in Table IV. From the results, we have the following observations. 1) Our method achieves better or comparable results than the other methods. This verifies the effectiveness of our method for early identification of Alzheimer’s disease. 2) The VoxCNN achieves good result. This is consistent with related studies [27], [43], implying a pretrained CNN (with AD/NC samples) is able to perform well on MCI tasks. Despite that, the proposed model still achieves comparable results and makes a balance between effectiveness

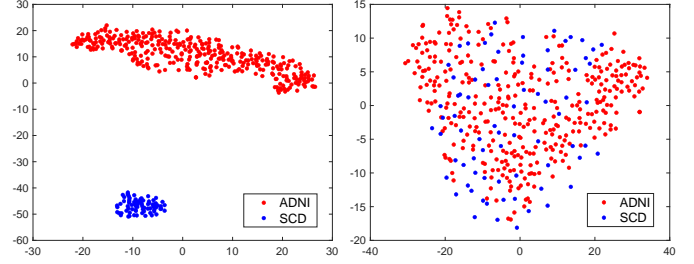


Fig. 4: Data distribution of the source (ADNI) and target data (SCD) before and after the domain adaptation processing.

and efficiency. 3) Compared with the results with SCD progression prediction, the proposed model achieves higher AUC value and more balanced SEN and SPE on MCI conversion task. This can be attributed to the much more training samples of MCI with relatively balanced positive/negative sample ratio.

VI. DISCUSSION

A. Data Distribution Visualization

We extract latent features of source data (ADNI) and target data (SCD) learned by the encoder after the adaptation training. The source and target data distribution of original ROI input and after adaptation is visualized using t-SNE [44], as shown in Fig. 4. From Fig. 4, these two domains have significant distribution differences in the original feature space. After adaptation, the proposed encoder is able to learn some shared features that can significantly decrease the domain shift between the two datasets.

B. Discriminative Brain Regions

It is helpful to identify a subset of biomarkers within the brain that are more closely linked to the prediction of SCD progression. Therefore, we investigate the top ten brain ROIs automatically identified by the attention module of our model in this work. We first aggregate the progressive SCD instances that have been correctly identified by our model. Then they are fed into the network and get their attention vectors which

TABLE IV: Performance of seven different methods for MCI-to-AD conversion prediction (*i.e.*, pMCI vs. sMCI classification).

Method	ACC (%)	BAC (%)	AUC (%)	SEN (%)	SPE (%)	$p < 0.05$
Baseline	64.12	64.04	69.20	63.47	64.60	Yes
TCA	60.56	60.71	62.24	61.68	59.73	Yes
GFK	65.14	64.92	70.08	63.47	66.37	Yes
SA	65.14	64.92	70.09	63.47	66.37	Yes
CORAL	64.38	64.26	69.84	63.47	65.04	Yes
VoxCNN	70.51	69.89	74.74	80.61	59.18	Yes
Ours	68.19	68.75	70.63	72.46	65.04	—

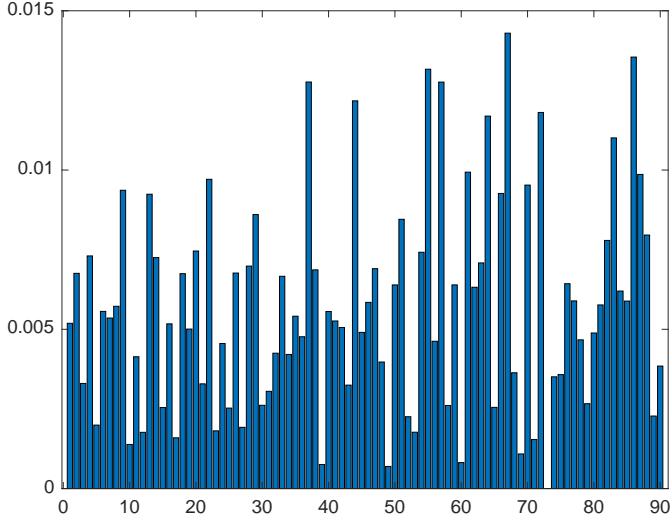


Fig. 5: Discriminative power (weights) of different brain ROIs outputted by the attention module in our model for progressive SCD identification.

TABLE V: Ten discriminative brain ROIs for progressive SCD identification selected by the attention module of our model.

Index	ROI Name	Related Studies
67	Precuneus left	[48]
86	Middle temporal gyrus right	[53]
55	Fusiform gyrus left	[54]
37	Hippocampus left	[49]
57	Postcentral gyrus left	[55]
44	Calcarine fissure right	[56]
72	Caudate nucleus right	[57]
64	Supramarginal gyrus right	[58]
83	Temporal pole left	[59]
61	Inferior parietal left	[60]

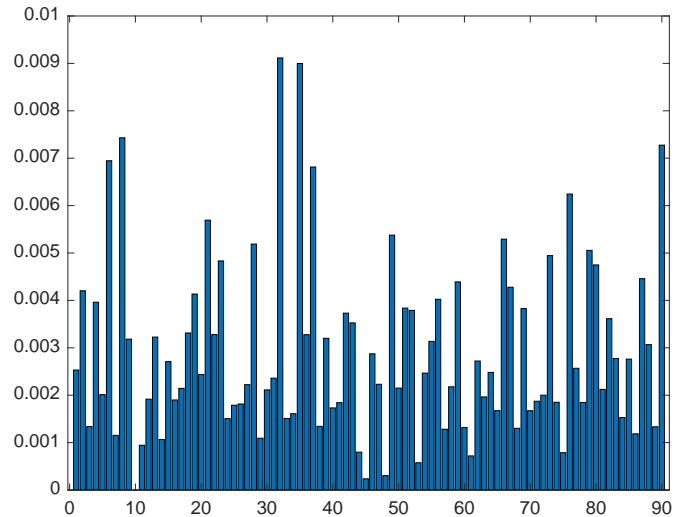


Fig. 6: Discriminative power (weights) of different Brain ROIs outputted by the attention module in our model for MCI-to-AD conversion prediction.

are computed by the attention module. Each element in the attention vector reflects the corresponding feature importance. The mean value of the attention vectors is used to indicate the brain region contribution (for visualization, we also minus the minimum value of the vector for each element). The selected ROIs that are more significant than others for the pSCD identification is visualized in Fig. 5. We also list the top ten brain regions that are selected by our model in Table V.

From Table V, we can observe that the most informative brain regions include precuneus, hippocampus and certain gyrus areas. In previous studies these brain regions are reported to be associated with the Alzheimer's disease [45]–[48]. For example, the precuneus has been recently emphasized as a key brain area for the memory impairment observed in early stage of AD [47], [48]. In addition, we also find an interesting phenomenon from our results that the progressive SCD is more closely linked with the left brain areas rather than the right part. This has also been found by some related studies [8].

We also visualize the importance of different ROIs for pMCI/sMCI classification as shown in Fig. 6 and list the top ten ROIs in Table VI. The identified areas mainly lie in certain gyrus and hippocampus areas which are consistent with some prior studies [49]–[52].

C. Ablation Study

To investigate the classification performance with other MRI features, we further use CNN features as the input of the proposed model, and test its performance for pSCD/sSCD classification. Specifically, we use a 3D CNN which is pre-trained with brain MRIs from other data sources as the feature extractor. Then the 3D CNN extracts features of the source data (AD/NC samples) and target data (SCD samples), respectively. The learned features are then fed into our model for adaptation and classification. In practice, we adopt a widely-used 3D VGG-Net CNN for brain MRI classification network, *i.e.*, VoxCNN [41]. It is pretrained with 205 AD and 231 NC samples acquired from other independent subjects in

TABLE VI: Ten discriminative brain ROIs (using the AAL atlas) for MCI conversion prediction selected by the attention module of our model.

ID	ROI Name	Related Studies
32	Anterior cingulate, paracingulate gyri right	[50]
35	Posterior cingulate gyrus left	[51]
8	Middle frontal gyrus right	[55]
90	Inferior temporal gyrus right	[52]
6	Superior frontal gyrus	[61]
37	Hippocampus left	[49]
76	Lenticular nucleus, pallidum right	[62]
21	Olfactory cortex left	[63]
49	Superior occipital gyrus left	[64]
66	Angular gyrus right	[65]

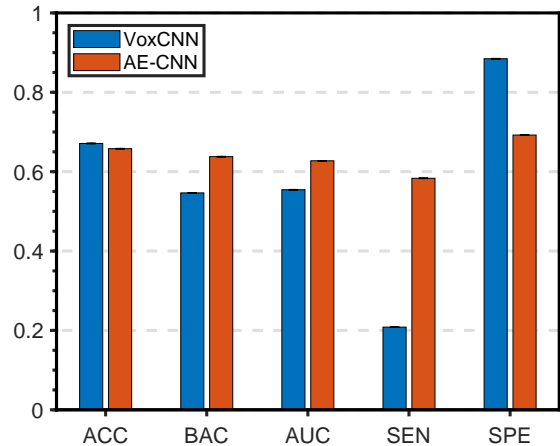
ADNI. The network involves 10 convolution layers, and the embeddings from the last activation of the convolution layer are used as the CNN feature. The dimension of CNN feature is 256. We also apply VoxCNN to pSCD/sSCD classification, and compare the result with our method, as shown in Fig. 7a. From the result, it can be seen that the proposed model outperforms the CNN in most cases. The CNN model has a trend of overfitting to the negative samples (sSCD) whereas our model is able to achieve a much more balanced accuracy. This indicates that a CNN trained with AD/NC samples cannot achieve good transferability to the task of SCD progression prediction.

In addition, we also compare the proposed model with ROI features and CNN features, as shown in Fig. 7b. From the results, the model with CNN features achieves higher AUC values while ROI features enables the model to achieve higher classification accuracy. Overall, their performance are comparable without dominant advantages over each other in SCD progression prediction.

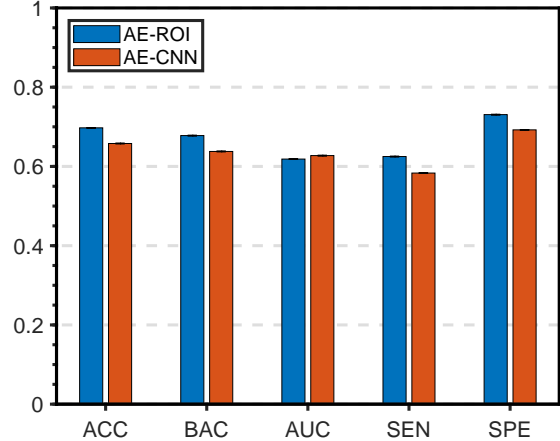
D. Parameter Analysis

1) *Influence of Dimension of Latent Space*: The encoder in our model plays the role of projecting source and target data into a shared latent space. Since this space is a compressed representation of the original features, the dimension of latent space is tunable. We explore the influence of this dimension and calculate the AUC values under different dimensions. The result is reported in Fig. 8. From the results, it can be observed that the model can achieve relatively good classification performance when the dimension of latent space is between 10~40. This implies that low-dimension spaces can be explored for cross-domain adaptation in the task of SCD progression prediction.

2) *Influence of Losses*: There are three losses for our model training as shown in Eq. 4. Since the target data (SCD) number is very small, the reconstruction loss \mathcal{L}_{recon} plays an important role for reflecting the information of target data. Thus we fix this parameter to 1 in Eq. 4 for the reconstruction loss, and vary the values of λ_1 and λ_2 to explore the their influences. Specifically, we independently change the values of λ_1 and λ_2 from 0.001, 0.01, 0.02, 0.05, 0.1, 0.2, 0.5, 1, and compute the corresponding AUC values for the pSCD/sSCD classification task. The result is reported in Fig. 9.



(a) Performance comparison of VoxCNN and our model with CNN features in the task of SCD progression prediction.



(b) Performance comparison of the proposed model with ROI features and CNN features for the task of SCD progression prediction.

Fig. 7: Ablation study of the proposed model with CNN features.

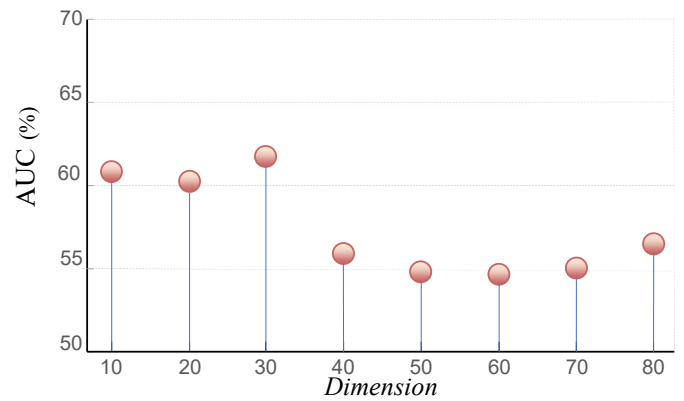


Fig. 8: Influence of dimension of the latent feature space on the pSCD/sSCD classification.

From Fig. 9, we have the following observations. First, When the λ_2 is quite small (≤ 0.02), the overall classification performance in terms of AUC is not good. This indicates the importance of the classification module in our model. When its contribution is reduced, the model will lose dis-

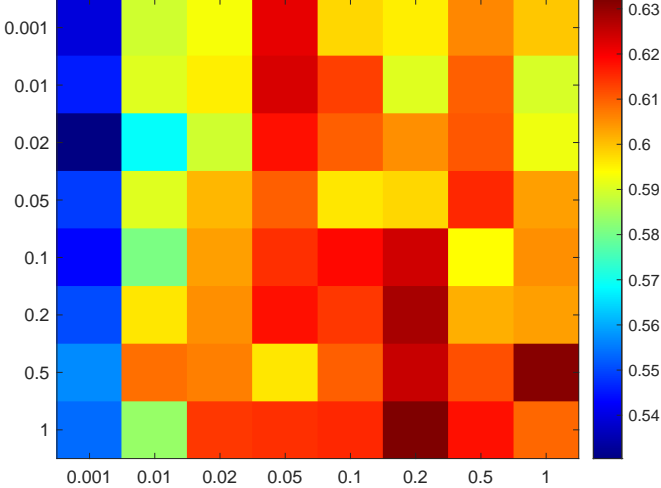


Fig. 9: Influence of the parameter of λ_1 (Y-axis) and λ_2 (X-axis) on the pSCD/sSCD classification in terms of AUC values.

crimination towards brain diseases. Second, in most cases, the classification performance with respect to λ_1 and λ_2 is stable, which demonstrates that our model is not very sensitive to parameters.

VII. CONCLUSION

In this paper, we propose an attention-guided autoencoder model for cross-domain MRI adaptation and SCD progression prediction. Our model takes brain ROI features as the input. An attention module helps enhance the overall performance and automatically find the most discriminative brain disease related regions. The joint training of a classification and a reconstruction modules help project the source and target data into a shared latent space where adaptation can be facilitated. From the experimental results, our model has three advantages: 1) good performance on small-sample-sized datasets which has extensive applications in medical imaging; 2) good interpretability which can help analyze disease-related brain areas with different brain atlases; 3) simple architecture and fast training/running speed. It only takes 5~10 seconds on CPUs to train and test the model with reproducible results. In the future, we intend to incorporate multi-modality features into our framework for further analysis.

REFERENCES

- [1] M. Goedert and M. G. Spillantini, "A century of Alzheimer's disease," *Science*, vol. 314, no. 5800, pp. 777–781, 2006.
- [2] F. Jessen *et al.*, "A conceptual framework for research on subjective cognitive decline in preclinical Alzheimer's disease," *Alzheimer's & Dementia*, vol. 10, no. 6, pp. 844–852, 2014.
- [3] L. A. Rabin *et al.*, "Subjective cognitive decline in preclinical Alzheimer's disease," *Annual review of clinical psychology*, vol. 13, pp. 369–396, 2017.
- [4] X. Wang *et al.*, "Neuroimaging advances regarding subjective cognitive decline in preclinical Alzheimer's disease," *Molecular Neurodegeneration*, vol. 15, no. 1, pp. 1–27, 2020.
- [5] A. F. Parker *et al.*, "A systematic review of neuroimaging studies comparing individuals with subjective cognitive decline to healthy controls," *Journal of Alzheimer's Disease*, pp. 1–23, 2022.
- [6] C. R. Jack Jr *et al.*, "The Alzheimer's Disease Neuroimaging Initiative (ADNI): MRI methods," *Journal of Magnetic Resonance Imaging*, vol. 27, no. 4, pp. 685–691, 2008.
- [7] E. E. Bron *et al.*, "Standardized evaluation of algorithms for computer-aided diagnosis of dementia based on structural MRI: The CADDementia challenge," *NeuroImage*, vol. 111, pp. 562–579, 2015.
- [8] L. Yue *et al.*, "Prediction of 7-year's conversion from subjective cognitive decline to mild cognitive impairment," *Human Brain Mapping*, vol. 42, no. 1, pp. 192–203, 2021.
- [9] A. Felpete *et al.*, "Predicting progression in subjective cognitive decline (scd) using a machine learning (ml) approach: The role of the complaint's severity: Neuropsychology/early detection of cognitive decline with neuropsychological tests," *Alzheimer's & Dementia*, vol. 16, 2020.
- [10] H. Lin *et al.*, "Identification of subjective cognitive decline due to Alzheimer's disease using multimodal MRI combining with machine learning," *Cerebral Cortex*, 2022.
- [11] Y. Liu *et al.*, "Assessing clinical progression from subjective cognitive decline to mild cognitive impairment with incomplete multi-modal neuroimages," *Medical Image Analysis*, vol. 75, p. 102266, 2022.
- [12] N. V. Chawla *et al.*, "SMOTE: synthetic minority over-sampling technique," *Journal of Artificial Intelligence Research*, vol. 16, pp. 321–357, 2002.
- [13] P. Chlap *et al.*, "A review of medical image data augmentation techniques for deep learning applications," *Journal of Medical Imaging and Radiation Oncology*, vol. 65, no. 5, pp. 545–563, 2021.
- [14] K. Engedal *et al.*, "The power of eeg to predict conversion from mild cognitive impairment and subjective cognitive decline to dementia," *Dementia and Geriatric Cognitive Disorders*, vol. 49, no. 1, pp. 38–47, 2020.
- [15] A. X. Pereiro *et al.*, "Relevance of complaint severity in predicting the progression of subjective cognitive decline and mild cognitive impairment: a machine learning approach," *Journal of Alzheimer's Disease*, vol. 82, no. 3, pp. 1229–1242, 2021.
- [16] G. Mirzaei, A. Adeli, and H. Adeli, "Imaging and machine learning techniques for diagnosis of Alzheimer's disease," *Reviews in the Neurosciences*, vol. 27, no. 8, pp. 857–870, 2016.
- [17] M. Tanveer *et al.*, "Machine learning techniques for the diagnosis of Alzheimer's disease: A review," *ACM Transactions on Multimedia Computing, Communications, and Applications*, vol. 16, no. 1s, pp. 1–35, 2020.
- [18] V. Cheplygina *et al.*, "Not-so-supervised: a survey of semi-supervised, multi-instance, and transfer learning in medical image analysis," *Medical image analysis*, vol. 54, pp. 280–296, 2019.
- [19] J. M. Valverde *et al.*, "Transfer learning in magnetic resonance brain imaging: A systematic review," *Journal of imaging*, vol. 7, no. 4, p. 66, 2021.
- [20] S. J. Pan and Q. Yang, "A survey on transfer learning," *IEEE Transactions on Knowledge and Data Engineering*, vol. 22, no. 10, pp. 1345–1359, 2009.
- [21] H. Guan and M. Liu, "Domain adaptation for medical image analysis: a survey," *IEEE Transactions on Biomedical Engineering*, vol. 69, no. 3, pp. 1173–1185, 2022.
- [22] G. Csurka *et al.*, *Domain adaptation in computer vision applications*. Springer, 2017.
- [23] B. Cheng *et al.*, "Domain transfer learning for mci conversion prediction," *IEEE Transactions on Biomedical Engineering*, vol. 62, no. 7, pp. 1805–1817, 2015.
- [24] ———, "Multi-domain transfer learning for early diagnosis of alzheimer's disease," *Neuroinformatics*, vol. 15, no. 2, pp. 115–132, 2017.
- [25] N. M. Khan *et al.*, "Transfer learning with intelligent training data selection for prediction of Alzheimer's disease," *IEEE Access*, vol. 7, pp. 72 726–72 735, 2019.
- [26] A. Mehmood *et al.*, "A transfer learning approach for early diagnosis of Alzheimer's disease on MRI images," *Neuroscience*, vol. 460, pp. 43–52, 2021.
- [27] C. Lian *et al.*, "Hierarchical fully convolutional network for joint atrophy localization and Alzheimer's disease diagnosis using structural mri," *IEEE Transactions on Pattern Analysis and Machine Intelligence*, vol. 42, no. 4, pp. 880–893, 2018.
- [28] S. Xiao *et al.*, "The China longitudinal ageing study: overview of the demographic, psychosocial and cognitive data of the Shanghai sample," *Journal of Mental Health*, vol. 25, no. 2, pp. 131–136, 2016.
- [29] N. Tzourio-Mazoyer *et al.*, "Automated anatomical labeling of activations in SPM using a macroscopic anatomical parcellation of the MNI MRI single-subject brain," *NeuroImage*, vol. 15, no. 1, pp. 273–289, 2002.
- [30] J. Pegueroles *et al.*, "Longitudinal brain structural changes in preclinical Alzheimer's disease," *Alzheimer's & Dementia*, vol. 13, no. 5, pp. 499–509, 2017.

[31] G. L. Wenk *et al.*, "Neuropathologic changes in Alzheimer's disease," *Journal of Clinical Psychiatry*, vol. 64, pp. 7–10, 2003.

[32] Y. Mu and F. H. Gage, "Adult hippocampal neurogenesis and its role in Alzheimer's disease," *Molecular Neurodegeneration*, vol. 6, no. 1, pp. 1–9, 2011.

[33] B. R. Ott *et al.*, "Brain ventricular volume and cerebrospinal fluid biomarkers of Alzheimer's disease," *Journal of Alzheimer's disease*, vol. 20, no. 2, pp. 647–657, 2010.

[34] D. L. Langer *et al.*, "Prostate cancer detection with multi-parametric MRI: Logistic regression analysis of quantitative T2, diffusion-weighted imaging, and dynamic contrast-enhanced MRI," *Journal of Magnetic Resonance Imaging*, vol. 30, no. 2, pp. 327–334, 2009.

[35] R. Divya and R. Shantha Selva Kumari, "Genetic algorithm with logistic regression feature selection for Alzheimer's disease classification," *Neural Computing and Applications*, vol. 33, no. 14, pp. 8435–8444, 2021.

[36] C. Wachinger *et al.*, "Domain adaptation for Alzheimer's disease diagnostics," *Neuroimage*, vol. 139, pp. 470–479, 2016.

[37] S. J. Pan *et al.*, "Domain adaptation via transfer component analysis," *IEEE Transactions on Neural Networks*, vol. 22, no. 2, pp. 199–210, 2010.

[38] B. Gong *et al.*, "Geodesic flow kernel for unsupervised domain adaptation," in *IEEE Conference on Computer Vision and Pattern Recognition*. IEEE, 2012, pp. 2066–2073.

[39] B. Fernando *et al.*, "Unsupervised visual domain adaptation using subspace alignment," in *Proceedings of the IEEE International Conference on Computer Vision*, 2013, pp. 2960–2967.

[40] B. Sun, J. Feng, and K. Saenko, "Return of frustratingly easy domain adaptation," in *Proceedings of the AAAI Conference on Artificial Intelligence*, vol. 30, no. 1, 2016.

[41] S. Korolev *et al.*, "Residual and plain convolutional neural networks for 3D brain MRI classification," in *14th IEEE International Symposium on Biomedical Imaging (ISBI)*, 2017, pp. 835–838.

[42] Y. Liu *et al.*, "Joint neuroimage synthesis and representation learning for conversion prediction of subjective cognitive decline," in *International Conference on Medical Image Computing and Computer-Assisted Intervention*. Springer, 2020, pp. 583–592.

[43] H. Guan *et al.*, "Learning transferable 3D-CNN for MRI-based brain disorder classification from scratch: An empirical study," in *International Workshop on Machine Learning in Medical Imaging*. Springer, 2021, pp. 10–19.

[44] L. Van der Maaten and G. Hinton, "Visualizing data using t-SNE," *Journal of Machine Learning Research*, vol. 9, no. 11, 2008.

[45] F. Lin *et al.*, "Insula and inferior frontal gyrus' activities protect memory performance against Alzheimer's disease pathology in old age," *Journal of Alzheimer's Disease*, vol. 55, no. 2, pp. 669–678, 2017.

[46] A. L. Foundas *et al.*, "Atrophy of the hippocampus, parietal cortex, and insula in Alzheimer's disease: a volumetric magnetic resonance imaging study," *Neuropsychiatry, Neuropsychology, & Behavioral Neurology*, 1997.

[47] G. Karas *et al.*, "Precuneus atrophy in early-onset Alzheimer's disease: a morphometric structural MRI study," *Neuroradiology*, vol. 49, no. 12, pp. 967–976, 2007.

[48] G. Koch *et al.*, "Transcranial magnetic stimulation of the precuneus enhances memory and neural activity in prodromal Alzheimer's disease," *Neuroimage*, vol. 169, pp. 302–311, 2018.

[49] F. Shi *et al.*, "Hippocampal volume and asymmetry in mild cognitive impairment and Alzheimer's disease: Meta-analyses of MRI studies," pp. 1055–1064, 2009.

[50] J. Tao *et al.*, "Mind-body exercise improves cognitive function and modulates the function and structure of the hippocampus and anterior cingulate cortex in patients with mild cognitive impairment," *NeuroImage: Clinical*, vol. 23, p. 101834, 2019.

[51] I. H. Choo *et al.*, "Posterior cingulate cortex atrophy and regional cingulum disruption in mild cognitive impairment and Alzheimer's disease," *Neurobiology of Aging*, vol. 31, no. 5, pp. 772–779, 2010.

[52] S. W. Scheff *et al.*, "Synaptic loss in the inferior temporal gyrus in mild cognitive impairment and Alzheimer's disease," *Journal of Alzheimer's Disease*, vol. 24, no. 3, pp. 547–557, 2011.

[53] J. S. Krasuski *et al.*, "Volumes of medial temporal lobe structures in patients with Alzheimer's disease and mild cognitive impairment (and in healthy controls)," *Biological Psychiatry*, vol. 43, no. 1, pp. 60–68, 1998.

[54] F. Z. Yetkin *et al.*, "fMRI of working memory in patients with mild cognitive impairment and probable Alzheimer's disease," *European Radiology*, vol. 16, no. 1, pp. 193–206, 2006.

[55] H. Yang *et al.*, "Study of brain morphology change in Alzheimer's disease and amnestic mild cognitive impairment compared with normal controls," *General Psychiatry*, vol. 32, no. 2, 2019.

[56] J. Ulrich, "Alzheimer changes in nondemented patients younger than sixty-five: Possible early stages of Alzheimer's disease and senile dementia of Alzheimer type," *Annals of Neurology: Official Journal of the American Neurological Association and the Child Neurology Society*, vol. 17, no. 3, pp. 273–277, 1985.

[57] K. Persson *et al.*, "Finding of increased caudate nucleus in patients with Alzheimer's disease," *Acta Neurologica Scandinavica*, vol. 137, no. 2, pp. 224–232, 2018.

[58] Y. Grignon *et al.*, "Cytoarchitectonic alterations in the supramarginal gyrus of late onset Alzheimer's disease," *Acta Neuropathologica*, vol. 95, no. 4, pp. 395–406, 1998.

[59] S. E. Arnold *et al.*, "Neuropathologic changes of the temporal pole in Alzheimer's disease and Pick's disease," *Archives of Neurology*, vol. 51, no. 2, pp. 145–150, 1994.

[60] S. J. Greene *et al.*, "Subregions of the inferior parietal lobule are affected in the progression to Alzheimer's disease," *Neurobiology of Aging*, vol. 31, no. 8, pp. 1304–1311, 2010.

[61] M. D. Ikonomovic *et al.*, "Superior frontal cortex cholinergic axon density in mild cognitive impairment and early Alzheimer disease," *Archives of Neurology*, vol. 64, no. 9, pp. 1312–1317, 2007.

[62] P. Liu *et al.*, "Gut microbiota interacts with intrinsic brain activity of patients with amnestic mild cognitive impairment," *CNS Neuroscience & Therapeutics*, vol. 27, no. 2, pp. 163–173, 2021.

[63] J. Djordjevic *et al.*, "Olfaction in patients with mild cognitive impairment and Alzheimer's disease," *Neurobiology of Aging*, vol. 29, no. 5, pp. 693–706, 2008.

[64] J. A. Matias-Guiu *et al.*, "Neural basis of cognitive assessment in Alzheimer disease, amnestic mild cognitive impairment, and subjective memory complaints," vol. 25, no. 7, pp. 730–740, 2017.

[65] D. F. Benson *et al.*, "Angular gyrus syndrome simulating Alzheimer's disease," vol. 39, no. 10, pp. 616–620, 1982.